論文 A Classification Method between Shear and Bond Splitting Failure Modes for Reinforced Concrete Beams

Primo Allan ALCANTARA[*1] and Hiroshi IMAI[*2]

ABSTRACT: Failure mode classification in reinforced concrete beams is especially difficult for brittle failure types such as shear and bond splitting. In this study, a new approach in the classification of the resulting failure mode is presented wherein emphasis is placed on the analysis of the main bar strain distribution based on the truss and arch model theory. Failure mode prediction from the proposed method is compared with experimental data from a number of beam specimens and showed good results. Also, an analysis on the ultimate strength of reinforced concrete beams is given.
KEYWORDS: reinforced concrete beam, failure mode classification, shear capacity, bond splitting capacity, truss and arch model

1. INTRODUCTION

Failure in reinforced concrete beams is classified into three major types, namely, shear, bond splitting and flexure. Conventional classification methods include the observation of the crack patterns, yielding of the steel reinforcement and load-displacement relationships. However, difficulty occurs when features of more than one type of failure mode are exhibited, especially for brittle types such as shear and bond splitting. Hence, a supplementary approach, which considers the strain distribution on the main reinforcement, is proposed. Analysis is based on the truss and arch model being the shear resisting mechanism of the beam.

2. EXPERIMENTAL PROCESS

In this study, a series in a number of beam experiments, which focused on the evaluation of the main bar post-insertion system[1)], is considered. The selected specimens were of the brittle type in order to have a comparison between the shear and bond splitting failure modes. A total of 8 specimens, which are two-thirds scale of typical rectangular reinforced concrete beams, are tested and analyzed. The details and specimen variations are shown in Fig. 1 and Table 1. Each beam specimen was set under the loading apparatus shown in Fig. 2. These specimens were subjected to varying shear forces that were applied continuously in a cyclic manner producing anti-symmetric bending moment distribution. The lateral force was applied through the horizontal actuator while the level of the loading frame was maintained by the vertical actuators.

For the proper simulation of seismic behavior, each specimen was made to displace once at a drift angle R equal to ±1/800, then twice at R of ±1/400, ±1/200, ±1/100 and ±1/50, and again once at R equal to ±1/25. The drift angle is the ratio of the relative displacement of the upper and lower loading members to the beam length. Moreover, strain gauges were strategically positioned on both the main and shear reinforcing bars of the specimens. Main quantitative data that were considered

*1 Graduate School, University of Tsukuba, Member of JCI
*2 Institute of Engineering Mechanics, University of Tsukuba, Member of JCI

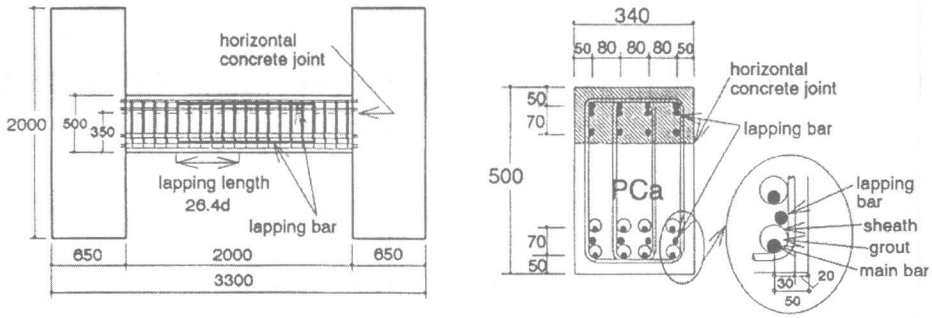

Fig. 1 Specimen Details

in this analysis are the actual strain in the steel reinforcement and the ultimate shear load attained. Besides these, qualitative observations from the resulting crack patterns were also considered.

Table 1 Specimen Specifications

Specimen	Stirrup	Grade (MPa)	Stirrup Ratio p_w (%)	$p_w\sigma_{wy}$ (MPa)
PCB-31	4-D10@70	SD295A	1.20	3.53
PCB-32	4-D10@80	SD345	1.05	3.60
PCB-33	4-D10@185	SD785	0.45	3.53
PCB-34	4-H7@170	USD1275	0.28	3.57
PCB-35	4-D10@140	SD295A	0.60	1.77
PCB-36	4-D10@140	SD345	0.60	2.06
PCB-37	4-D10@140	SD785	0.60	4.71
PCB-38	4-H7@80	USD1275	0.59	7.52

main bar: 8-D25(SD685) lapping bar: 4-D25(SD685)
sheath: 42mm diameter concrete: 33.3~35.3 MPa

3. ULTIMATE STRENGTH

The shear capacity of the beams was calculated using the strength equation given in the design code of the Architectural Institute of Japan[2], which is as shown in Eq. (1). This equation is based on the truss and arch model theory wherein the first term represents the contribution of the truss mechanism while the second term is for the arch mechanism.

$$Q_{su} = Q_{sut} + Q_{sua} = bj_t p_w \sigma_{wy} \cot\phi + \tan\theta(1-\beta)bD\nu\sigma_B / 2 \quad (1)$$

On the other hand, for the bond splitting capacity, the truss and arch model was also made as the basis of the shear resisting mechanism. Accordingly, the bond splitting capacity is given by Eq. (2), which is again composed of contributions of both the truss and arch mechanisms.

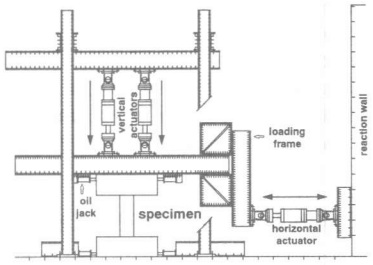

Fig. 2 Loading Apparatus

$$Q_{bu} = Q_{but} + Q_{bua} = \tau_{bu}(\Sigma\psi) j_t + \tan\theta(1-\beta)bD\nu\sigma_B / 2 \quad (2)$$

where τ_{bu} : bond strength of the main reinforcement; $\Sigma\psi$: summation of the perimeter of the extreme row of main reinforcement; $\beta = \{\tau_{bu}(\Sigma\psi)(1+\cot^2\phi)\}/(b\cot\phi\nu\sigma_B)$

The bond splitting capacity of beams is mainly dependent of the bond strength of the main reinforcement. For this study, the bond strength equation proposed by Kaku[3] would be considered since experimental tests on the main bar post-insertion system using sheaths show good estimates of the bond strength of the main bars. The bond strength for top cast main bars according to Kaku is represented by Eqs. (3) and (4) and is composed of contributions of both the concrete and the shear reinforcement. Moreover, for the precast concrete specimens, the diameter of the sheath represents the diameter of the main bar (d_b). Also, as for the presence of the lapping bars, studies[4] showed that the bond behavior of those with lapping bars is very much similar to that of a continuous main bar for beams using the main bar post-insertion system.

$$\tau_{bu} = [0.17 + 0.06b_i + 0.31k_n(qb_i + 18.2p_w b/(Nd_b))] \cdot \sqrt{\sigma_B} \quad (3)$$

but when $p_w\sigma_{wy} < 0.413\sqrt{\sigma_B}$,

$$\tau_{bu} = [0.42 + 0.14b_i + 0.76k_n(qb_i + 18.2p_w b/(Nd_b))] \cdot p_w\sigma_{wy} \quad (4)$$

With regard to the initial calculation of the bond splitting capacities of the beams using Eq. (2), results show a rather low estimate of the actual capacity. This is mainly due to the consideration of only the extreme row of main reinforcement in the calculation. Past research show that an additional contribution on the bond capacity is given by the second layer of main reinforcement. This contribution is represented by the concrete component of the bond strength of the main reinforcement since the second layer is not directly confined or restrained by the shear reinforcement. Considering the Kaku equation, the concrete component is shown in Eq. (5).

$$\tau_{co} = [0.17 + 0.06b_i] \cdot \sqrt{\sigma_B} \; or \; [0.42 + 0.14b_i] \cdot p_w\sigma_{wy} \quad (5)$$

Therefore, the terms in the truss mechanism component of the bond splitting capacity equation is adjusted to consider the second layer of main reinforcement and is given by Eq. (6). This modification considers the casting orientation (k_o =1.2) of the second layer bars as bottom cast bars.

$$\tau_{bu}(\Sigma\psi) \rightarrow \tau_{bu}(\Sigma\psi_1) + k_o\tau_{co}(\Sigma\psi_2) \quad (6)$$

4. TRUSS AND ARCH MODEL

The application of the truss and arch model in the determination of the strain distribution in the main reinforcement is considered. For both the shear and bond splitting failure modes, it is assumed that the level of straining in the main bars remains in the elastic range, and that, even though the bars are stressed under repeated loading, their behavior seems to be similar to that subjected to monotonic loading.

In the truss mechanism, the value of the strain is determined using the calculated force in the main bar based on the equilibrium of the infinitesimal stringer elements. Since the beam is loaded under double bending, it is considered as point symmetric at the center of the member. Hence, from the free body diagram shown in Fig. 3, since the stress condition at both points in the main reinforcement lying on a plane inclined at an angle ϕ passing through the center of the column is the same, it can be shown that the strain is zero at those same points in the main reinforcement. Moreover, since the force in the main bar is associated with stresses due to bond, it is directly dependent on the distance from the point of zero strain. Therefore, the resulting bond forces in the main bars for both the shear and bond splitting types are represented by Eqs. (7) and (8), respectively.

$$bond\ force = p_w\sigma_{wy} b \cot\phi\, l_x \quad \text{(shear type)} \quad (7)$$

$$bond\ force = \tau_{bu}\Sigma\psi\, l_x \quad \text{(bond splitting type)} \quad (8)$$

where l_x : distance from the point of zero strain

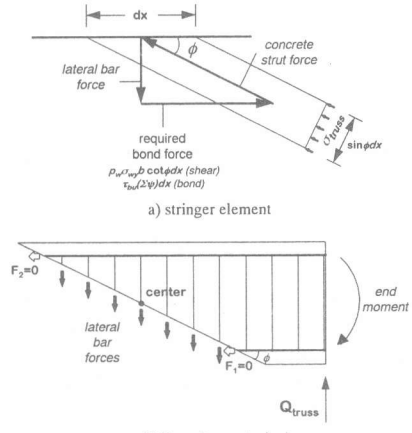

Fig. 3 Equilibrium Conditions

By converting the force to strain, the strain distribution due to the truss mechanism in terms of the calculated capacity, Q_{truss}, is given by Eq. (9).

$$\varepsilon_{truss} = \frac{Q_{truss} l_x}{j_t a_r E} \tag{9}$$

where $Q_{truss} = Q_{sut}$ (shear type) or $= Q_{but}$ (bond splitting type); a_r : total cross sectional area of the extreme row of main reinforcement; E : modulus of elasticity of the main reinforcement

A diagram showing the strain distribution due to the truss mechanism is provided in Fig. 4.

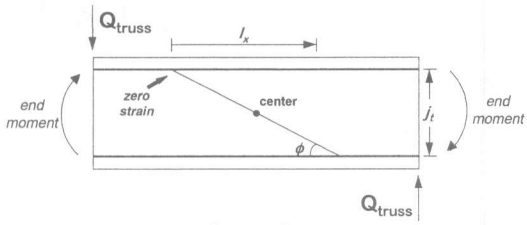

a) truss action

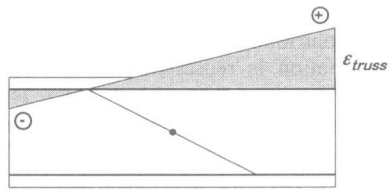

b) strain distribution

Fig. 4 Truss Mechanism

In the arch mechanism, the value of the strain is derived from the calculated compressive force in the concrete strut lying along the main diagonal of the beam. From Fig. 5 and by equilibrium, the compressive force in the concrete arch is converted to tensile forces in the main bars. Using the remaining compressive stress of the concrete for the arch mechanism, ${}_c\sigma_a$, the compressive force in the concrete arch is given by Eq. (10).

$$compressive\ force = \frac{{}_c\sigma_a bD/2}{\cos\theta} \tag{10}$$

By equilibrium, the resultant of the forces in all of the main bars is given by Eq. (11).

$$bar\ force = {}_c\sigma_a bD/2 \tag{11}$$

Therefore, the strain due to the arch mechanism in terms of the calculated capacity, Q_{arch}, is given by Eq. (12).

$$\varepsilon_{arch} = \frac{Q_{arch}}{\tan\theta\, a_g E} \tag{12}$$

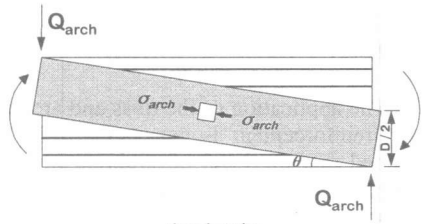

a) arch action

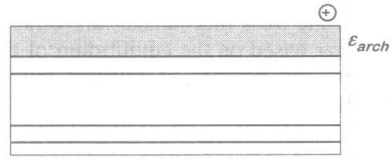

b) strain distribution

Fig. 5 Arch Mechanism

where $Q_{arch} = Q_{sua}$ (shear type) or $= Q_{bua}$ (bond splitting type); a_g : total cross sectional area of all the main bars

A diagram showing the strain distribution due to the arch mechanism is also provided in Fig. 5.

In the calculation of the strain on the extreme row of main reinforcement, it is necessary to consider the presence of inner main bars, for this case, the second layer of main reinforcement. Adjustment is made on the calculation of the strain contributed by the truss mechanism since proper consideration of the second layer of main bars was already given for the arch mechanism component. It is assumed that the shear force due to the truss mechanism can be divided into contributions by the first and the second layer of main reinforcement. A logical approach is by considering the bond strength calculation of the first or extreme row of main bars compared to that

of the second layer of main bars. In the calculation of the bond splitting capacity, the contribution given by the extreme row of main bars is determined by multiplying the calculated capacity due to the truss mechanism by a factor, α, as shown in Eq. (13).

$$\alpha = \frac{\tau_{bu}(\Sigma\psi_1)}{\tau_{bu}(\Sigma\psi_1) + k_o\tau_{co}(\Sigma\psi_2)} \tag{13}$$

In other words, the term Q_{truss} in Eq. (9) is multiplied by α showing the representative force contribution of the extreme row of main bars for both the shear and bond splitting failure modes. To summarize, the strain distribution in the extreme main bars is determined by Eq. (14).

$$\varepsilon = \varepsilon_{truss} + \varepsilon_{arch} = \frac{\alpha Q_{truss} l_x}{j_t a_r E} + \frac{Q_{arch}}{\tan\theta\, a_g E} \tag{14}$$

5. FAILURE MODE CLASSIFICATION

In the determination of the resulting failure mode in an actual scaled experimentation, the most basic method would be to rely on the crack patterns during the progress of testing. The location and orientation of the cracks as well as the crushing of the concrete is of great aid in the task of classifying the type of the resulting failure mode. Typical crack patterns of the shear and bond splitting failure modes at peak loading are shown in Fig. 6.

It can be observed from Fig. 6 that there is similarity in the crack patterns of the shear and bond splitting types. Therefore, there is great difficulty in the classification of the resulting failure mode since both shear and bond splitting cracks are present at failure or peak loading. In such cases, a further approach would be to consider the strain condition of the lateral reinforcement or stirrups. The shear mode is characterized by the yielding of the stirrups at failure while the bond splitting mode is normally depicted by a non-yielding condition. However, during the actual testing of the specimens, it is very difficult to perform a thorough observation on the time of appearance of the cracks, at the same time, on the strain behavior of the stirrups, during the short span before and after failure.

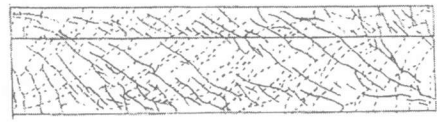

a) B32 Shear Failure Type

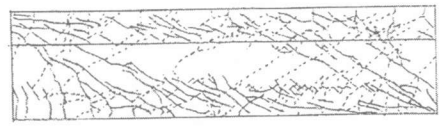

b) B34 Bond Failure Type

Fig. 6 Crack Patterns

To supplement the conventional methods of classification, an analysis on the state of stress along the main reinforcement is performed. Concepts given in sections 3 and 4 are utilized and comparisons between the experimental and theoretical strain distributions based on both types of failure modes are conducted. The theoretical lines according to the shear and bond splitting failure modes were derived using the truss and arch mechanisms with consideration of the presence of the second layer of main reinforcement. Also, it is assumed that the main bars remain in the elastic range during failure. Moreover, since the specimens considered are all of the precast type, the diameter of the sheath is used as the working value for the diameter of the main reinforcement in the calculation of the bond splitting capacity.

Before proceeding to the analysis of the main bar strain distribution, a discussion on the ultimate strength calculations is given. Aside from the shear and bond splitting capacities, a calculation on the flexural strength of the beams based on the e-function method is made. These theoretical strengths together with the actual experimental capacities are shown in Table 2. Results show that there is a generally good agreement between the predicted and actual failure modes with

the exception of specimens PCB-31 and PCB-32. This is dealt with in the next discussion on the main bar strain distribution.

Figure 7 shows plots of the actual and theoretical strain distributions of the extreme layer of main bars (top cast) for several specimens. Again, except for specimens PCB-31 and PCB-32, a good correspondence between the experimental and theoretical main bar strain distributions is observed whether it be of shear or bond splitting failure. This can be seen from Figs. 7 (b) and (c). With regard to Fig. 7 (a), specimen PCB-32 shows a strain level much less than the predicted strain at either shear or bond splitting failure. This is in agreement with the low capacity attained during the testing of the beam. Thus, it can be inferred that there is an overestimation of the theoretical capacities. To recapitulate, it is, therefore, confirmed that the different approach using the main bar strain distribution supplements the conventional methods in classifying failure modes for reinforced concrete beams. Also, the proposed classification method could assist in the proper evaluation of the ultimate strength capacities especially for shear and bond splitting types.

Table 2 Ultimate Strength

Specimen	Shear Strength	Bond Splitting Strength	Flexural Strength	Actual Strength	Predicted Failure Mode	Actual Failure Mode
PCB-31	1033	895	956	815	Bo	F/S
PCB-32	988	861	956	862	Bo	F/S
PCB-33	986	732	958	728	Bo	Bo
PCB-34	697	688	958	646	Bo	Bo
PCB-35	681	738	959	645	S	S
PCB-36	682	739	959	639	S	S
PCB-37	1097	779	959	738	Bo	Bo
PCB-38	1103	776	959	829	Bo	Bo

strengths in kN

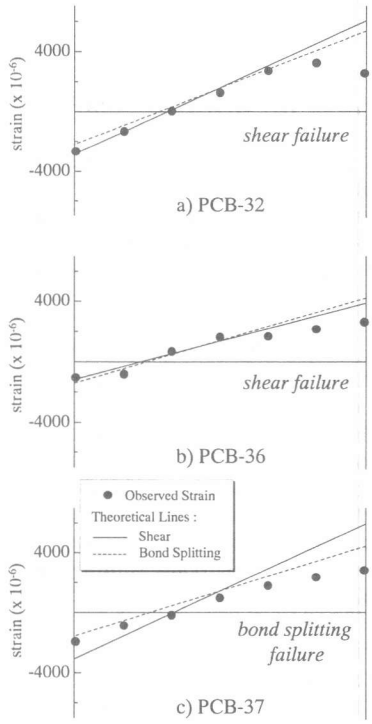

Fig. 7 Main Bar Strain Distribution (top cast bars)

6. CONCLUSIONS

This study focused on the determination of the resulting failure mode based on the truss and arch model theory. Using the experimental strains in the main reinforcement and with proper consideration of the second layer of main bars, it can be concluded that the failure classification between the shear and bond splitting modes is generally accurate. Moreover, it should be noted that the proposed classification method supports the validity of the use of the truss and arch mechanisms in the evaluation of the ultimate strengths of reinforced concrete beams.

REFERENCES

1) Imai, H., "Precast Method for Frame Type Buildings", Structural Failure Durability and Retrofitting, 1993, pp. 396-403.
2) AIJ, "AIJ Structural Design Guidelines for Reinforced Concrete Buildings", JCI, 1994, pp. 77-123.
3) Kaku, T., et al., "The Influence of Yield Stress of Transverse Reinforcement on the Bond Strength of Reinforced Concrete Members", Proceedings of the JCI, Vol. 16, No. 2, 1994, pp. 247-252.
4) Hatahira, A., "The Seismic Behavior of Precast Concrete Beams using High Strength Lateral Reinforcement", Master's Thesis, Doctoral Program of Engineering, University of Tsukuba, 1996.

ACKNOWLEDGEMENTS

The authors would like to express their deepest gratitude to Mr. Akitoshi Hatahira, formerly from the Graduate School of Engineering in the University of Tsukuba, for his great contribution on the analysis of this research work.